https://doi.org/10.5194/angeo-2019-91
Preprint. Discussion started: 8 July 2019

Annales Geophysicae Discussions
Open Access
EGU

Spatial and seasonal effects on the delayed ionospheric response to solar EUV changes

Erik Schmölter[1], Jens Berdermann[1], Norbert Jakowski[1], and Christoph Jacobi[2]

[1]German Aerospace Center, Kalkhorstweg 53, 17235 Neustrelitz, Germany
[2]Leipzig Institute for Meteorology, Universität Leipzig, Stephanstr. 3, 04103 Leipzig, Germany

Correspondence: Erik Schmölter (Erik.Schmoelter@dlr.de)

Abstract. This study correlates different ionospheric parameters with the integrated solar EUV radiation for an analysis of the delayed ionospheric response in order to confirm previous studies on the delay and to further specify variations of the delay. Several time series for correlation coefficients and delays are presented to characterize the trend of the delay from 2011 to 2013. The impact of the diurnal variations of ionospheric parameters in the analysis on hourly resolution for fixed locations are discussed and specified with calculations in different time scales and with comparison to solar and geomagnetic activity. An average delay for TEC of ≈ 18.7 hours and for foF2 of ≈ 18.6 hours is calculated at four European stations. Through comparison with the Australian region the difference between northern and southern hemisphere is analyzed and a seasonal variation of the delay between northern and southern hemisphere is calculated for TEC with $\approx 5 \pm 0.7$ hours and foF2 with $\approx 8 \pm 0.8$ hours. The latitudinal and longitudinal variability of the delay is analyzed for the European region and a decrease of the delay from ≈ 21.5 hours at $30°$N to ≈ 19.0 hours at $70°$N has been found. For winter months a roughly constant delay of ≈ 19.5 hours is calculated. In this study a North-South trend of the ionospheric delay during summer month has been observed with ≈ 0.06 hours per degree in latitude. The results based on solar and ionospheric data in hourly resolution and the analysis of the delayed ionospheric response to solar EUV show the seasonal and latitudinal variations. Results also indicate the dependence on the geomagnetic activity as well as on the 11-year solar cycle.

1 Introduction

The solar extreme ultraviolet radiation (EUV) is the dominating source of ionization in the ionosphere. Therefore, the high variability of EUV within the 27-day solar rotation cycle, the 11-year solar cycle, or within short-term events like solar flares (Berdermann et al., 2018) has a strong impact on the ionosphere. The resulting photoionization, together with photodissociation, recombination, and transport processes, causes different ionospheric variations, which can be time- or location-dependent. The structure of the ionosphere is dominated by the interaction of different wavelength ranges in the EUV spectrum with the respective particle population and composition in specific altitudes. This results in different ionospheric layers defined by the

https://doi.org/10.5194/angeo-2019-91
Preprint. Discussion started: 8 July 2019

Annales Geophysicae Discussions
Open Access
EGU

Publication	Delay [d]	Solar flux parameter	Ionospheric parameter
Titheridge (1973)	1	Mg II	Global mean TEC
Jakowski et al. (1991)	1-2	F10.7	TEC
Jakowski et al. (2002)	1-3	F10.7	TEC
Afraimovich et al. (2008)	1.5-2.5	F10.7, EUV	Global mean TEC
Oinats et al. (2008)	2-4	F10.7	NmF2, TEC
Zhang and Holt (2008)	2-3	F10.7	Electron density
Min et al. (2009)	2	F10.7	Electron density, TEC
Lee et al. (2012)	1-2	F10.7	Electron density
Jacobi et al. (2016)	1-2	F10.7, EUV	Global mean TEC
Ren et al. (2018)	1	EUV	Electron density

Table 1. The table presents results from former studies, which provide a first rough information (daily resolution) of the ionospheric delay to the solar activity.

density distribution of the ion species. An understanding of these chemical and physical processes in the ionosphere is important, since many modern navigation, communication, and land surveying applications rely on precise positioning based on Global Navigation Satellite Systems (GNSS). GNSS performance is strongly influenced by radio signal propagation through the dynamic ionosphere. Therefore, satellite navigation applications require realistic ionospheric models in order to predict ionospheric changes in high temporal and spatial resolution. The exact information on the electron content is needed which is needed to correct the ionospheric influence on GNSS positioning. Detailed knowledge about the ionospheric reaction to solar EUV can directly contribute to the improvement of ionospheric models and give a better understanding of the physical processes involved.

Former analyses of the ionospheric electron content changes in connection with solar flux variations, in particular on the 27-day rotation time scale, have revealed a delay of ionospheric parameters with respect to solar variability. A selection of studies is presented in Table 1. In these studies, the ionospheric delay was calculated based on different proxies and EUV flux data, with only a rough estimate ranging between one and three days (daily resolution).

In this study we analyze the delay in high temporal resolution. Furthermore, we give an overview about the expected variations in the delayed ionospheric response in the northern and southern hemisphere in general with an additional more detailed focus on the European region. This analysis is made based on GNSS and ionosonde data over Europe and Australia. Time series of the delays and the correlation coefficients are calculated between solar EUV radiation and two ionospheric parameters: the Total Electron Content (TEC) and the critical frequency of the F2 layer (foF2). TEC measures the vertical integrated electron density and can be used to describe changes in the whole ionosphere-plasmasphere system due to solar EUV variability. The availability of TEC in maps with good data coverage for certain regions (e.g. Europe) allows a spatial analysis of the delay and a comparison with the foF2 data for specific locations. On the other hand, foF2 describes only the F2 layer of the ionosphere

https://doi.org/10.5194/angeo-2019-91
Preprint. Discussion started: 8 July 2019

Annales Geophysicae Discussions

and there is no dependence to other regions in the upper atmosphere compared to TEC. Nevertheless, we will show that the results for the delay are very similar for both ionospheric parameters.

In preparation for the analysis, we discuss the problems and challenges of using data with hourly resolution and which impacts the diurnal variations in the ionospheric parameters have on the cross-correlations. This discussion is crucial for the interpretation of the calculated delays.

2 Data

Parts of the EUV spectrum has been continuously measured since the year 2000 and EUV observational data can be accessed from the Solar EUV Experiment (SEE) onboard the Thermosphere Ionosphere Mesosphere Energetics and Dynamics (TIMED) satellite (Woods et al., 2005), the Geostationary Operational Environmental Satellites (GOES) (Machol et al., 2016), or the Solar Auto-Calibrating EUV/UV Spectrophotometers (SolACES) (Nikutowski et al., 2011; Schmidtke et al., 2014). The data used in this paper are from the Solar Dynamics Observatory (SDO) EUV Variability Experiment (EVE) (LASP, 2019). They represent almost the whole EUV spectrum (wavelength range from 0.1 to 105 nm with a spectral resolution of 0.1 nm) and have the required high resolution of at least one hour for the delay analysis (temporal resolution of 20 seconds). EVE data also cover a long time period (2011 to 2014) without large data gaps (Woods et al., 2012).

In the analysis, we correlate EUV with two important ionospheric parameters, appropriate to investigate the processes responsible for the ionospheric delay. The first and most important parameter is TEC, which is well suited for the analysis of the ionospheric response to solar EUV variations. TEC is an integral measurement of the electron density and less sensitive to disturbances, such as plasma redistribution, than other parameters. The time series of TEC for single locations and regions is extracted from the International GNSS Service (IGS) TEC maps (NASA, 2019b), which provide coverage since 1998 with the required high resolution of at least one hour (Hernández-Pajares et al., 2009). These TEC data represent a weighted average between real observations and an ionospheric model, dependent on the availability of observations at a given time and location. In preparation for calculating the delay, TEC values at seven ionosonde locations and one region (Europe) were resampled from the TEC maps, where the values of the nearest grid point were extracted for each location.

The other ionospheric parameter included in the analysis, foF2, is derived from ionosonde station data (NOAA, 2019) provided by the National Oceanic and Atmospheric Administration (NOAA), and are available for the same time periods with high temporal resolution (Wright and Paul, 1981). Figure 1 shows a map of stations used to calculate the ionospheric delay. The geographic and geomagnetic latitudes and longitudes of the stations are shown in Table 2. In the northern hemisphere, the European stations Tromsø, Průhonice, Rome, and Athens were selected, since they cover different latitudes ranging from $\approx 38°$N to $\approx 70°$N. The dense coverage of GPS stations over Europe allows a good comparison with TEC data for these locations. An analysis of the southern hemisphere with the South African region would be preferred because of a similar longitude, but there are some time and data gaps, which prevented a reliable estimation of the delay for the available stations. Instead we use data from the Australian stations Darwin, Camden, and Canberra for the analysis in the southern hemisphere. These stations cover latitudes between $\approx 12°$S to $\approx 35°$S. The variability of the characteristic ionosphere parameter foF2

https://doi.org/10.5194/angeo-2019-91
Preprint. Discussion started: 8 July 2019

Annales Geophysicae Discussions
Open Access
EGU

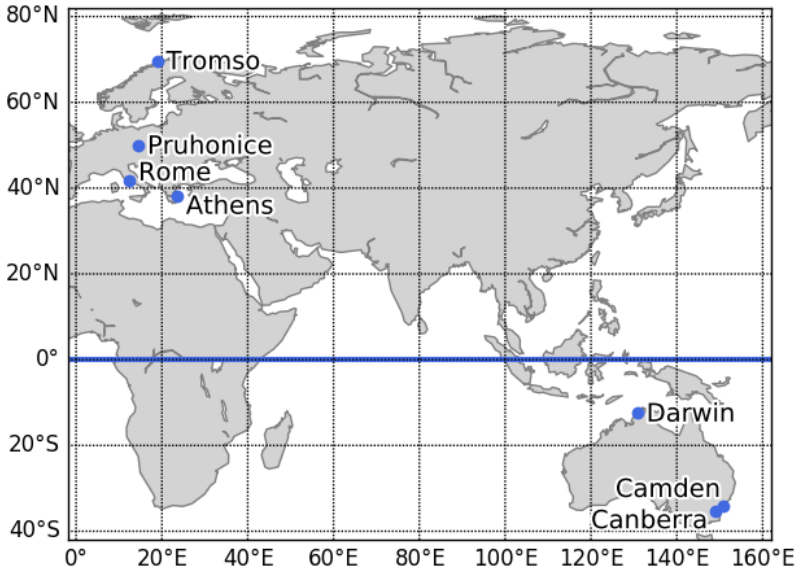

Figure 1. The European (Tromsø, Průhonice, Rome and Athens) and Australian (Darwin, Camden, Canberra) ionosonde stations which are used in the calculation of the delayed response of the ionosphere to solar EUV variations.

Station	geographic [°]		geomagnetic [°]	
	Lat.	Lon.	Lat.	Lon.
Tromsø	69.7	19.0	67.0	117.5
Průhonice	50.0	14.6	49.7	98.5
Rome	41.8	12.5	42.3	93.2
Athens	38.0	23.6	36.4	102.5
Darwin	-12.4	130.9	-22.9	-157.3
Camden	-34.0	150.7	-42.0	-132.4
Canberra	-35.3	149.0	-43.7	-134.3

Table 2. Geographic and geomagnetic latitudes and longitudes of the European (Tromsø, Průhonice, Rome and Athens) and Australian (Darwin, Camden, Canberra) ionosonde stations which are used in the calculation of the delayed response of the ionosphere to solar EUV variations.

https://doi.org/10.5194/angeo-2019-91
Preprint. Discussion started: 8 July 2019

measured with ionosondes are compared to the EUV flux. In preparation of the analysis, all data are resampled to an hourly resolution and gaps are filled with a linear interpolation. Unlike in Schmölter et al. (2018), there are no band-stop filters to reduce the daily variations, since this calculation step does not add more reliability to the delay calculation. The Kp-index (NASA, 2019a) is used to characterize the influence of the geomagnetic activity on the delay in the analysis.

3 Correlation of ionospheric parameters with solar EUV

The delayed ionospheric response to solar variability was calculated by different studies in daily resolution. A selection of these studies are shown in Table 1. A first delay calculation with cross-correlations in hourly resolution was done by Schmölter et al. (2018). Here we extend previous research by addressing daily and seasonal as well as regional dependencies of the ionospheric delay in high temporal resolution. In the analysis different locations are compared and corresponding time series for ionospheric parameters include different variations: diurnal variations, 27-day solar rotation cycle, seasonal variations. Figure 2 shows the impact of the diurnal variations on the correlation coefficients by comparing different temporal resolutions (weekly, daily, hourly). The TEC data in hourly resolution are extracted from IGS TEC maps at the location of Rome ($\approx 41.8°$N and $\approx 12.5°$E). The EUV data are integrated SDO-EVE fluxes from 6 to 105 nm. The daily and weekly data sets for TEC are retrieved by calculating the corresponding means for the values from 11:00 to 13:00 each day, i.e. only the time periods with an expected maximum photoionization are considered. The correlation coefficients between EUV and TEC data are calculated using a time window of approximately 90 days. The comparison of correlation coefficients in hourly and weekly resolution in Figure 2 shows that the correlation on hourly resolution is, as expected, much smaller. Increases and decreases of the correlation coefficients have the same trend though. A characterization of the correlation trend is possible in all shown resolutions.

In Figure 3 the correlation coefficients and delay between TEC and EUV are shown for a fixed location (Rome with a latitude of $\approx 41.8°$N and a longitude of $\approx 12.5°$E) and a fixed local time (12:00) at the same latitude ($40°$N). The correlation coefficients and delay for both results are calculated with cross-correlations using a time window of approximately 90 days with the TEC and EUV data. The difference between both methods is the extraction of the TEC time series from the TEC maps. For the calculation with fixed location the latitude and longitude are unchanged for each data point. For the calculation with fixed local time the longitude is changed to correspond with the location at 12:00 local time. In Figure 3 the differences of the correlation coefficients are shown. The correlation coefficients for a fixed local time are greater than for a fixed location, but strong increases or decreases of the trend appear in both data sets (e.g. the strong decreases in the end of 2011 and 2012). The trend of the delay with a slight increase over the three years as well as the annual variation are present. The impact of the diurnal variation on the trend of the delay is negligible for a characterization.

The analysis with fixed local time is not used in the further analysis, since the extracted time series from the IGS TEC maps relies less on measurements considering areas with few or no ground stations. The time series have a certain dependence on the underlying model (for the chosen IGS TEC maps by Universitat Politècnica de Catalunya (UPC), a global voxel-defined 2-layer tomographic model solved with Kalman filter and spline interpolation). Despite of the strong diurnal variations in the ionospheric parameters and their impact on the correlation and the delay calculation, Figures 2 and 3 show, that relative

https://doi.org/10.5194/angeo-2019-91
Preprint. Discussion started: 8 July 2019

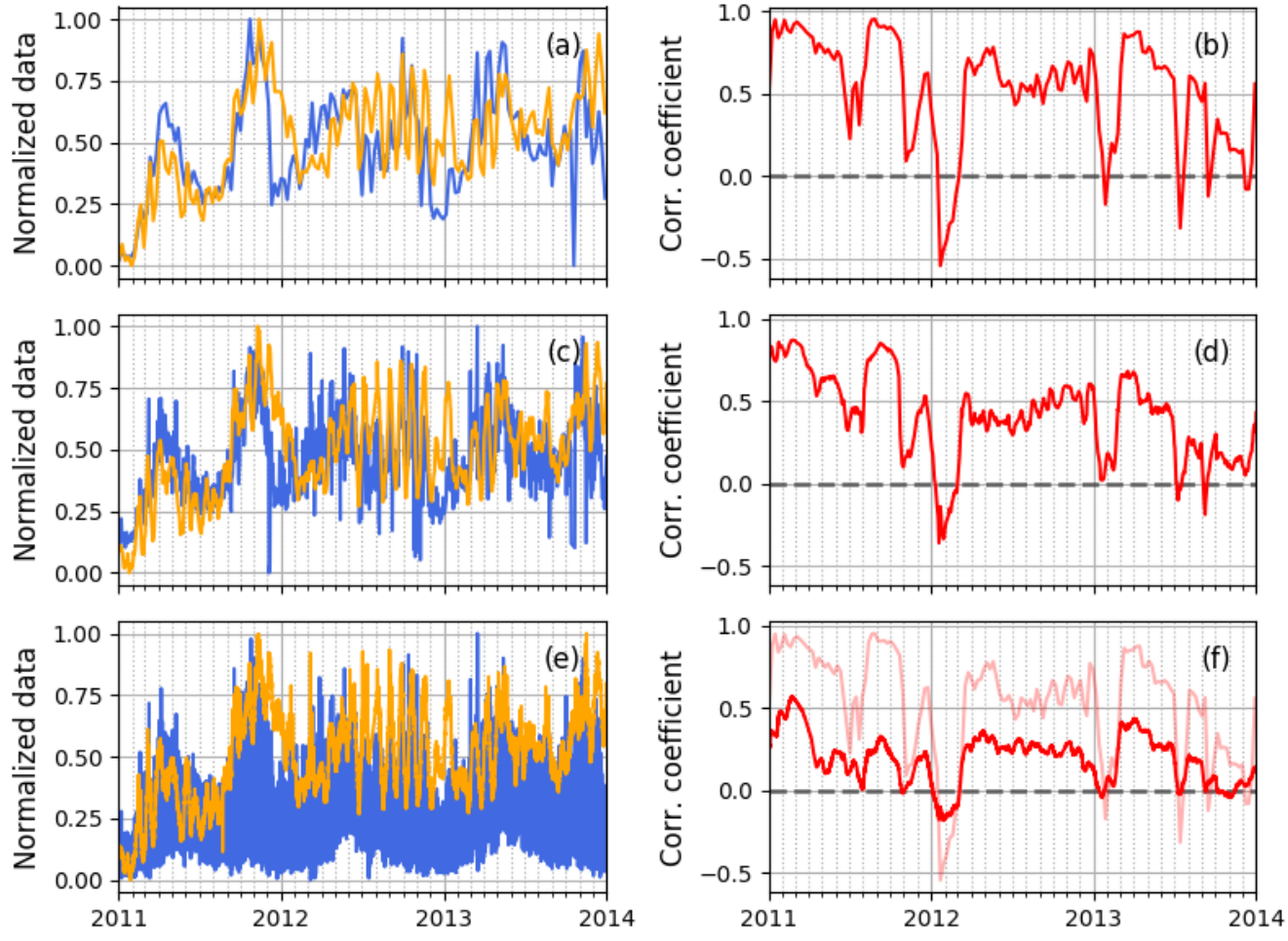

Figure 2. The plot show the normalized TEC (blue) and EUV (orange) data as well as the resulting correlation coefficients (red) for different temporal resolutions: weekly (a, b), daily (c, d) and hourly resolution (e, f). The correlation coefficients were calculated using a time window of approximately 90 days and a step size corresponding to each resolution. The daily and weekly TEC data were retrieved by calculating the mean for the values from 11:00 to 13:00 local time each day. The correlations coefficients for the weekly resolution are shown in the plot for the hourly resolution again (light red). All data correspond to the location of Rome with $\approx 41.8°$N and $\approx 12.5°$E.

trends can be calculated in hourly resolutions for fixed locations. The significant decreases of the correlation and the negative correlation coefficients are not effects of the diurnal variations, since they are in the same order for all results and the observed trend must have another origin (see Figures 2 and 3).

Geomagnetic activity and thermospheric conditions have an additional impact on the ionospheric state as well. In the chosen time period from 2011 until 2014 for this study (during a solar minimum) a stronger impact of the geomagnetic activity can be expected (Zieger and Mursula, 1998). These variations are not covered by EUV flux measurements and cannot be characterized

https://doi.org/10.5194/angeo-2019-91
Preprint. Discussion started: 8 July 2019

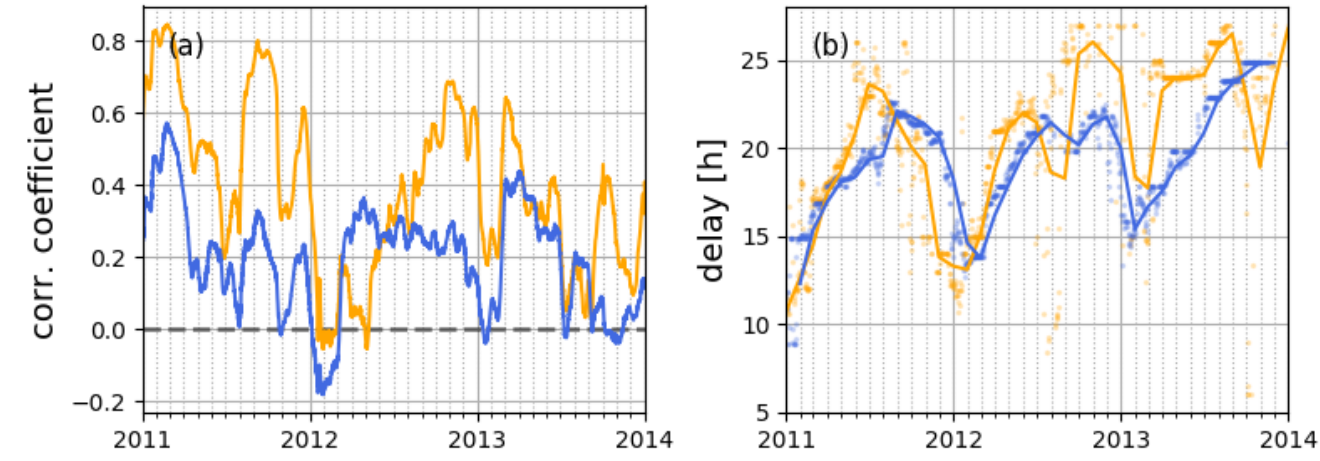

Figure 3. Plot (a) shows the correlation coefficients and plot (b) the delays calculated with a fixed location (blue) and a fixed local time (orange). The fixed location is Rome ($\approx 41.8^{\circ}$N and $\approx 12.5^{\circ}$E) and the fixed local time is 12:00 at 40°N. The correlation coefficients and delays were calculated using a time window of approximately 90 days and a step size of 1 hour with TEC and EUV data. The delays in hourly resolution are shown by dots and the monthly means of the delays are shown as solid lines.

with the cross-correlations between solar EUV and ionospheric parameters. In Figure 4 the calculated correlation coefficients and delay from the location Rome (already shown in Figure 3) are compared to the Kp-index as a measure of the geomagnetic activity. The smoothed trends of the Kp-index, correlation coefficient between EUV and TEC as well as delay between EUV and TEC show similar decreases in all three data sets during the end of each year. The minimum of the correlation coefficient and the delay are about two month behind the minimum of the Kp-index. The strong impact of the geomagnetic activity on the delay was reported e.g. by Ren et al. (2018), and Figure 4 gives a first indication about such a relation. In the further analysis, we will show similar results for the southern hemisphere, confirming this behavior as a global trend in the mid-latitudes.

In conclusion, the results in Figures 2, 3 and 4 show that the diurnal variations have a impact on the correlation between EUV and TEC on hourly resolution. We do not see any significant changes in the trend and get information about different variations. In the following analysis we will characterize certain variations, while keeping in mind, that their magnitude might be several values off due to the deviations caused by the diurnal variations.

4 Representation of the delay for TEC and foF2

In earlier studies, the correlation of the ionospheric delay has been calculated for different ionospheric parameters based on daily or hourly resolutions, as shown in Table 1. Jakowski et al. (1991), for example, used the solar radio flux index F10.7 and calculated a delay of one to two days. Jacobi et al. (2016) confirmed this delay with satellite-based EUV-TEC measurements and also calculated the delay with EVE fluxes, because proxies like F10.7 or EUV-TEC (Unglaub et al., 2011) are not able to

https://doi.org/10.5194/angeo-2019-91
Preprint. Discussion started: 8 July 2019

Annales Geophysicae Discussions
Open Access
EGU

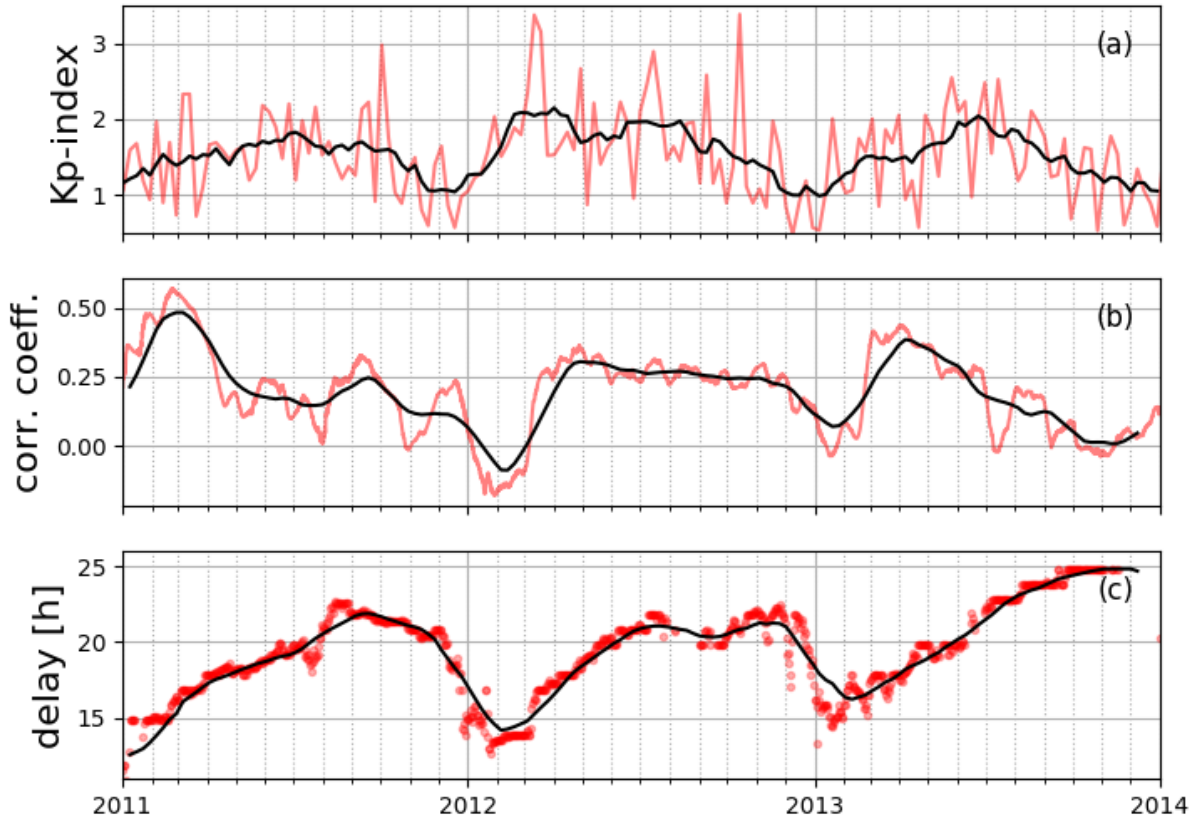

Figure 4. Kp-index (a), correlation coefficient between EUV and TEC (b), delay between EUV and TEC (c). In each plot the transparent red line or dots show the raw data and the black line weekly means to present the overall trend. All data correspond to the location of Rome with $\approx 41.8°$N and $\approx 12.5°$E.

cover all ionospheric effects. In addition, the solar rotation variations of F10.7 and EUV are not synchronized at all times and the calculated delay with F10.7 might be greater than the actual delayed ionospheric response to EUV (Woods et al., 2005; Chen et al., 2018). Schmölter et al. (2018) used EVE and GOES EUV fluxes to calculate an ionospheric delay of about 17 hours as mean value based on data at hourly time resolution.

We would like to confirm these results and extend the analysis by correlating the integrated EVE fluxes for the whole EUV spectrum (from 6 to 105 nm) with the relevant ionospheric parameters TEC and foF2. Furthermore, we investigate similarities and differences of the ionospheric delay using data from both hemispheres and provide temporal and regional dependencies. In the calculation, a time window of 90 days and a step length of one hour are used for the cross-correlations. This time frame not

https://doi.org/10.5194/angeo-2019-91
Preprint. Discussion started: 8 July 2019

Annales Geophysicae Discussions
Open Access
EGU

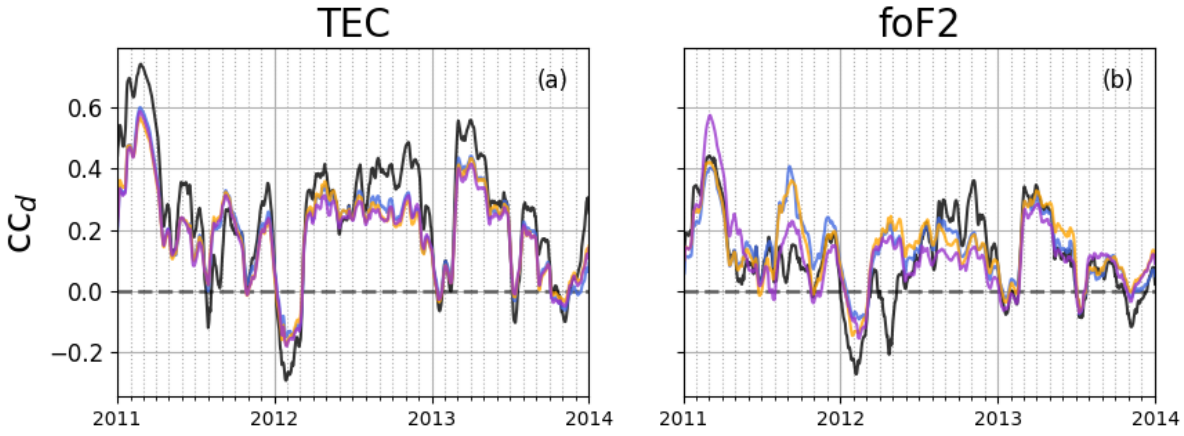

Figure 5. The plots show the correlation coefficients of the ionospheric parameters TEC (a) and foF2 (b) with integrated EVE fluxes (6 to 105 nm) for Tromsø (black), Průhonice (blue), Rome (orange), and Athens (purple). All parameters were analyzed in hourly resolution using a time window of 90 days and a step size of one hour.

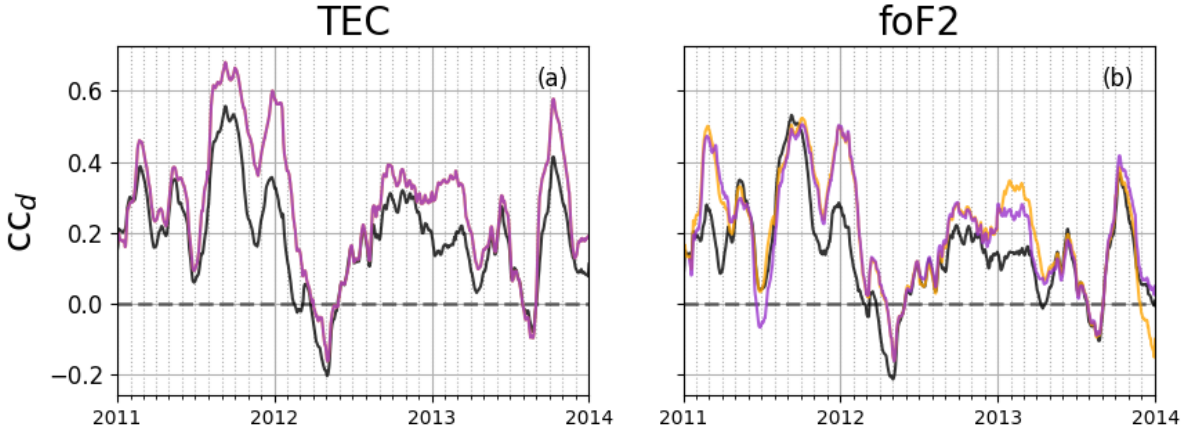

Figure 6. The plots show the correlation coefficients of the ionospheric parameters TEC (a) and foF2 (b) with integrated EVE fluxes (6 to 105 nm) for Darwin (black), Camden (orange), and Canberra (purple). All parameters were analyzed in hourly resolution using a time window of 90 days and a step size of one hour.

only allows to produce reliable results for the delay, it also allows to identify changes in the delay over time. The calculation is applied to the time series from December 2010 to February 2014 and covers a time period of roughly three years.

The results for the European stations are shown in Figure 5 for TEC and foF2. The trend of the correlation coefficients of TEC for the four European stations are very similar. The station Tromsø has more significant peaks (for increases and decreases in the correlation), but follows the same general trend. At the end of each year the correlation decreases significantly and

https://doi.org/10.5194/angeo-2019-91
Preprint. Discussion started: 8 July 2019

reaches negative values, which was already seen in Figure 4 as a possible effect of the geomagnetic activity. At the end of the chosen time period the correlation gets especially low, which is due to data gaps and the applied interpolation. The correlation coefficients of foF2 for the four European stations are smaller than for TEC. The results show a similar trend compared to correlation coefficients of TEC and are similar for the different stations. The correlation coefficients for the station Tromsø show again the largest deviation from the mean of the trends of the other stations. Since Tromsø is an auroral station, the processes in the ionosphere for this location are influenced by other mechanisms, e.g., particle precipitation or thermospheric heating controlled by the solar wind (Hunsucker and Hargreaves, 2002). We still include this station in the analysis of the delayed ionospheric response as the northern boundary for the European region.

The results for the Australian stations for TEC and foF2 are shown in Figure 6. In general, the correlation coefficients of TEC and foF2 are slightly larger than for the European stations. The trend of correlation coefficients for both parameters and the trend for the different stations are in good agreement. The suggested impact of the geomagnetic activity is less present in these results, and especially the decrease and minimum in December 2012 does not occur. The difference might be due to further impacts on the correlation, e.g. thermospheric conditions or seasonal variations not covered in this study, but which are known to have a strong impact on the ionospheric state (Rishbeth, 1998; Rishbeth et al., 2000).

The results of the delay calculation through cross-correlations are shown in Figure 7 and 8. The trend of the delay for TEC and foF2 at the European stations in Figure 7 is in agreement with the trend found by Schmölter et al. (2018), having a slow increase in the delay during the first half of the year, a maximum of the delay close to the end of the year and a sudden decrease of the delay at the end of the year. This pattern repeats in the three years of the chosen time period. The trend of the delay for TEC and foF2 at the Australian stations in Figure 8 is very similar, but shows a less linear increase of the delay in each year. Contrary to the correlation coefficients in the Figures 5 and 6, the delays show a good correlation with the geomagnetic activity in both hemispheres. Hence, this global trend confirms an additional dependence of the delay on the geomagnetic activity.

The maxima of the delay increase from year to year in 2011 to 2013 (especially for foF2) in the northern hemisphere. A similar trend occurs in the southern hemisphere from 2011 to 2012. This small increase might result from the growing solar activity in the same time period. Figure 9 shows the data for integrated EUV during the analyzed time period and the calculated delay for TEC at Rome and Canberra. As a very coarse visualization for the correlation between EUV and delay, the linear trends in both data sets are shown as well. The long-term trends of EUV and the delay on the northern and southern hemisphere increase within the chosen time period. Thus, during the solar maximum (cycle 24), long-term changes in the EUV seem to correlate with variations in the delay. A similar behavior was suggested by Schmölter et al. (2018) based on an analysis using GOES data for the same time period. Rich et al. (2003) indicated a smaller delay for solar minimum and a longer delay for solar maximum, and Chen et al. (2015) found a decrease in the trend of the delay with decreasing solar activity. Both analyses calculated the delay only in daily resolution but on longer time periods.

As seen in Figures 5 and 6, the delays for the European and Australian stations do not show an obvious difference with respect to seasonal variations due to the global trend, which has to be removed in the further analysis. Therefore, we picked the European station Rome with a latitude of $\approx 42°$N (geomagnetic latitude $\approx 42°$N) and the Australian station Canberra with a latitude of $\approx 35°$S (geomagnetic latitude $\approx 43°$S) for the comparison of the northern and southern hemispheres. In our

https://doi.org/10.5194/angeo-2019-91
Preprint. Discussion started: 8 July 2019

Annales Geophysicae Discussions
Open Access
EGU

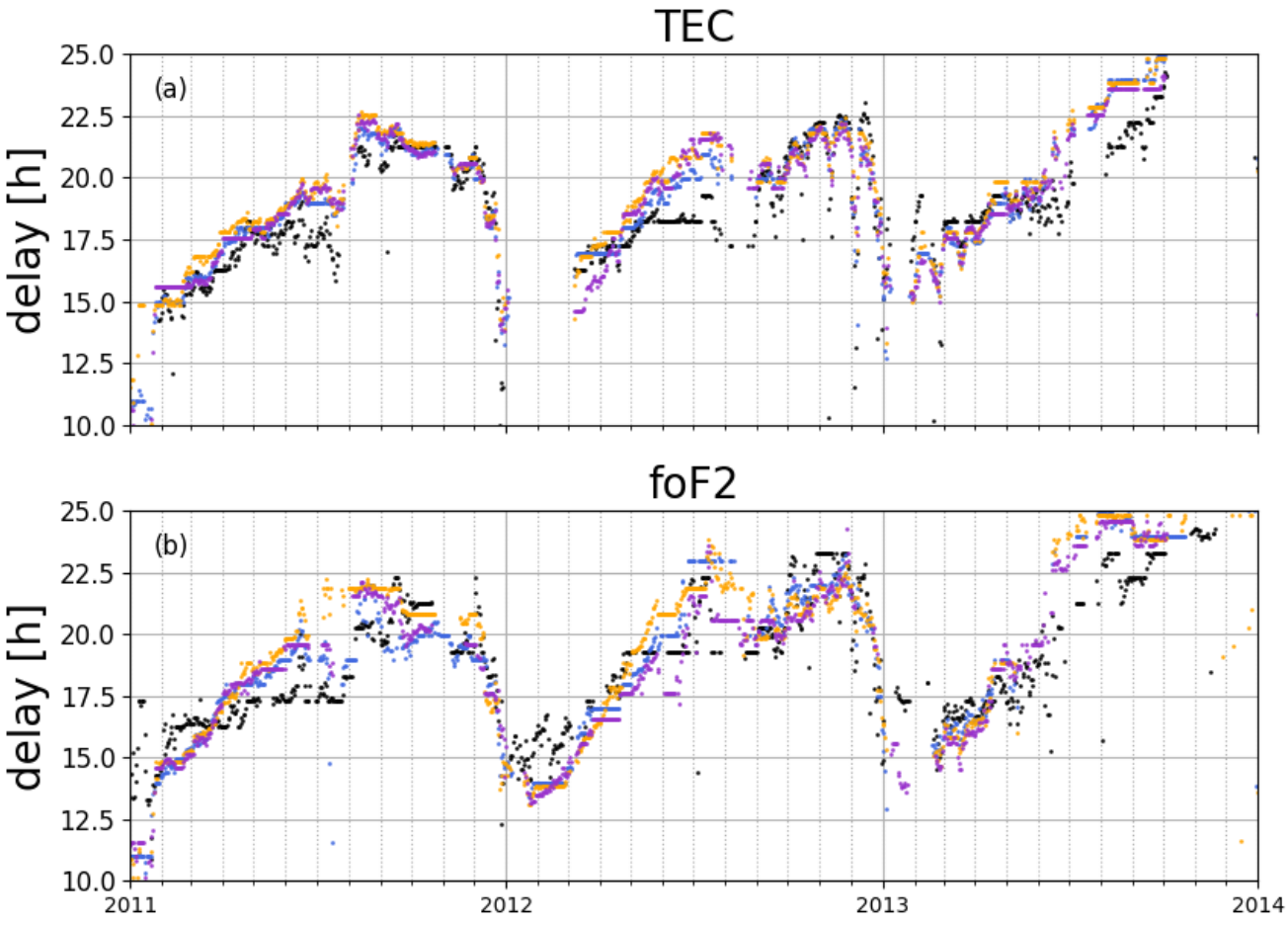

Figure 7. The plots show the delays of the ionospheric parameters TEC (a) and foF2 (b) with integrated EVE fluxes (6 to 105 nm) for Tromsø (black), Průhonice (blue), Rome (orange), and Athens (purple). All parameters were analyzed in hourly resolution using a time window of 90 days and a step size of one hour.

analysis we indirectly eliminated the global trend by calculating the difference between the delays calculated at both stations. The results are shown in Figure 10. The difference between both stations clearly shows a seasonal variation in the northern and southern hemisphere with a greater delay for Rome in the northern hemisphere summer and a greater delay for Canberra in the southern hemisphere summer. The delay difference varies over different ranges for the parameters: TEC with $\approx 5 \pm 0.7$ hours and foF2 with $\approx 8 \pm 0.8$ hours. These results indicate a strong seasonal variation of the ionospheric delay in the F2 layer compared to the whole ionosphere-plasmasphere system. Similar to the discussion of the impact of diurnal variations, such findings need to be confirmed with modeling efforts. In conclusion, the trends of the ionospheric delay for TEC and foF2 are very similar and both ionospheric parameters show features of the seasonal variations.

https://doi.org/10.5194/angeo-2019-91
Preprint. Discussion started: 8 July 2019

Annales Geophysicae Discussions
Open Access
EGU

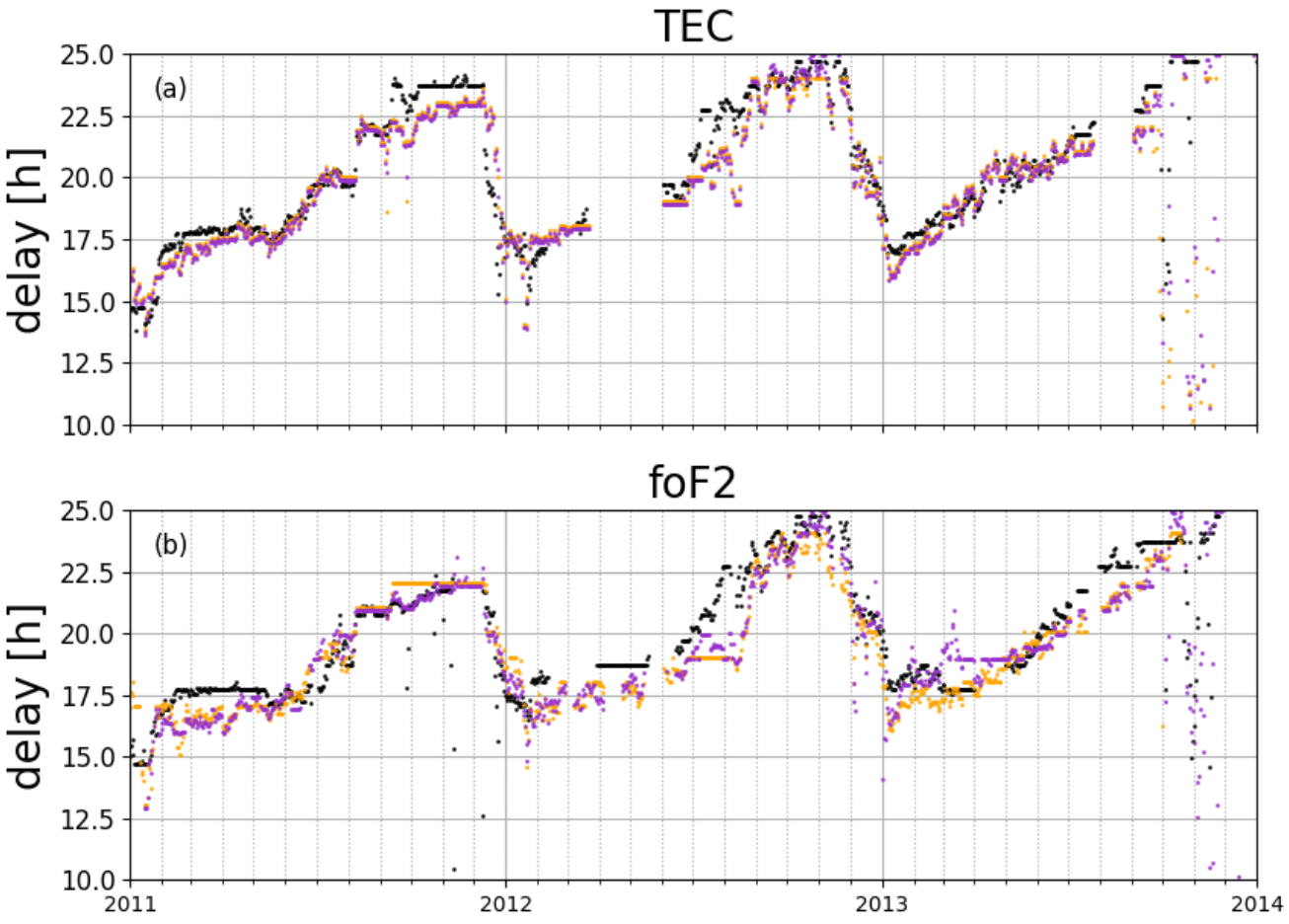

Figure 8. The plots show the delays of the ionospheric parameters TEC (a) and foF2 (b) with integrated EVE fluxes (6 to 105 nm) for Darwin (black), Camden (orange), and Canberra (purple). All parameters were analyzed in hourly resolution using a time window of 90 days and a step size of one hour.

5 Analysis of the delay for mid-latitudes

Another trend visible in Figure 7 is a decrease of the delay with latitude in summer. The station Tromsø shows the shortest delay of the European stations for both parameters. The differences in the delay between Průhonice, Rome, and Athens are smaller. The different delay between Tromsø and the other European stations is expected due to the explained differences in the auroral region. The latitudinal dependence is not visible during winter. No such trend is visible for the Australian stations and there are only minimal differences in the delay. This is probably due to the smaller range of latitudes covered by this stations, where data from high-latitudes are missing. A precise interpretation of the trend without data from different latitudes in the southern hemisphere is difficult. Nonetheless, the results for the latitudes over Europe agree with the expectations that different

https://doi.org/10.5194/angeo-2019-91
Preprint. Discussion started: 8 July 2019

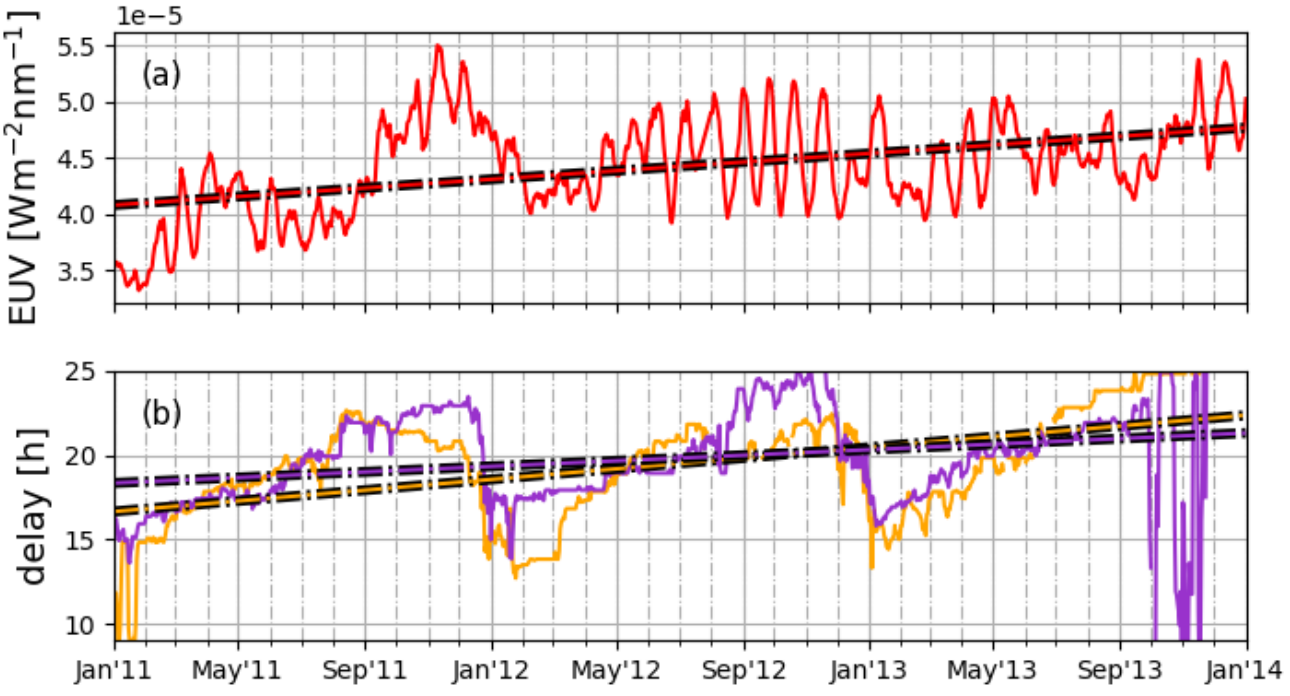

Figure 9. Plot (a) shows the the integrated EUV fluxes from 6 to 105 nm and the linear trend of the EUV (dash-dotted line). Plot (b) shows the delays of TEC against EUV for Rome (orange) and Canberra (purple), as well as the linear trends of the delays (dash-dotted lines).

and more varying delays can be observed in polar regions due to the direct impact of the solar wind as well as for the equatorial region due to the strong dynamics between the different ionospheric layers.

A further analysis of the mid-latitude delay is possible using TEC data over Europe, where we have good observation coverage from GNSS stations and only minimal influence by the ionospheric model (for the chosen IGS TEC maps by UPC: a global voxel-defined 2-layer tomographic model solved with Kalman filter and spline interpolation). Therefore, we are able to extract a region from the TEC maps (30°N to 70°N and 10°W to 30°E) and calculate the time series of the delay for each available grid point. This was done by cross-correlations with a time window of 90 days and a step length of one hour. For the results in Figure 11, which shows a map of delay values for the mid-latitudes in summer and winter, the mean and standard deviation from May to August and from November to February were calculated. The maps in Figure 11 show that the delay is consistent with the results from the European ionosonde stations. In winter, there is no strong increase or decrease with latitude, but roughly the same delay of ≈ 19.5 hours for the whole region. A slight decrease at the northern and southern boundary support the statement, that the delay is decreasing at polar and equatorial regions. A similar behavior of the delay has been found by Ren et al. (2018). In summer, the delay decreases with latitude from ≈ 21.5 hours at 30°N to ≈ 19 hours at 70°N. The gradient in summer describes a change of ≈ -0.06 hours per degree in latitude. Therefore, the delay maps confirm

https://doi.org/10.5194/angeo-2019-91
Preprint. Discussion started: 8 July 2019

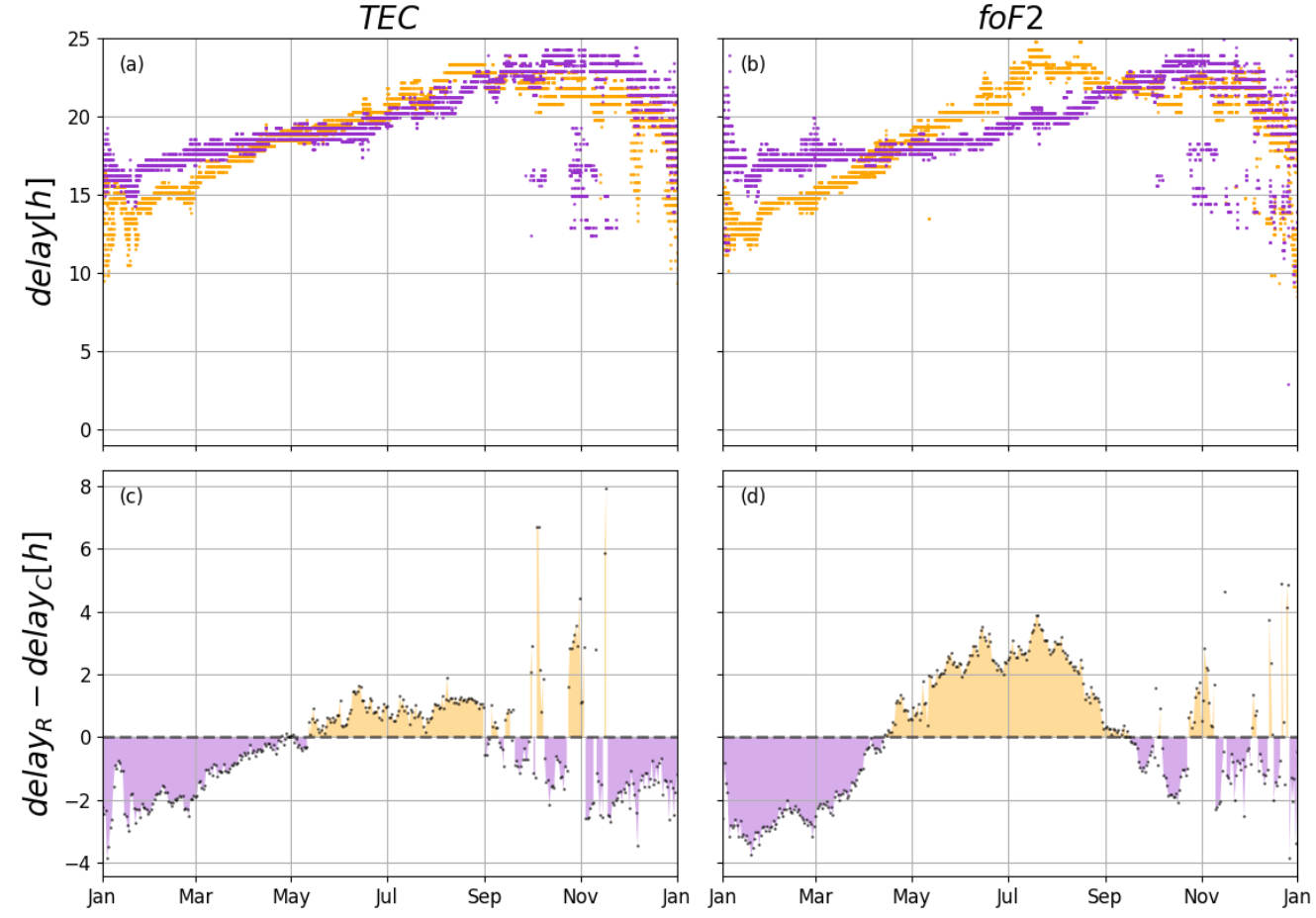

Figure 10. Superposed epoch plots for the delay (a, b) and difference in delays (c, d) for the ionospheric parameters TEC and foF2 with integrated EVE fluxes (6 to 105 nm) for Rome (orange) and Canberra (purple). The temporal resolution is one hour.

the latitudinal variations as seen in Figure 7. The variation in delay with longitude is small and does not show any dominant trend in winter. The variation of the delay with longitude in summer is much smaller than in latitude with a change of ≈ -0.01 hours per degree in longitude.

For the further analysis the calculated time series of delay maps is averaged over longitude to get a mean value for the delay at each latitude. The results are summarized with epoch plots in Figure 12 having a resampled resolution of one week to allow better presentation of the long-term changes of the ionospheric delay. The latitude-dependent time series in Figure 12 is consistent with the results and the assumed trend from the seasonal variations is present. In October, the delay reaches the same value for all latitudes and does not change any more until the sudden decrease in December, which happens for all latitudes. A global trend based on the geomagnetic activity is as well represented in Figure 12.

https://doi.org/10.5194/angeo-2019-91
Preprint. Discussion started: 8 July 2019

Annales Geophysicae Discussions
Open Access
EGU

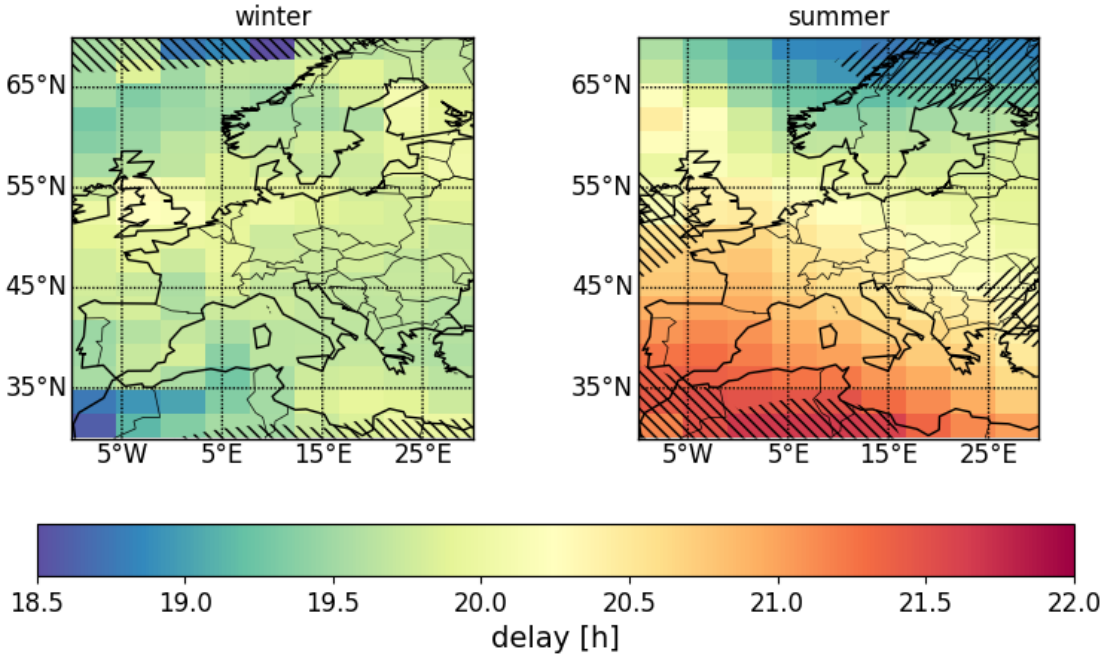

Figure 11. Map of the delay of TEC with respect to EUV in summer (May to August) and winter (November to February) within the time period from 2011 to 2014. The delay varies between ≈ 18.6 and ≈ 21.7 hours. The hatched regions on the map represent significantly greater (upper left to lower right fill) or smaller (upper right to lower left fill) correlations compared to the average of each map ($\pm$ one standard deviation).

6 Conclusions

The main challenge of delay calculation in high temporal resolution is the impact of the diurnal variations of ionospheric parameters. These have a impact on the calculated correlations coefficients, but do not influence the relative trend in a significant way. We proved that a reliable delay calculation is possible on hourly resolution by different analysis: comparison of delays between fixed local time and fixed location as well as comparison of correlation coefficients on different time scales. These results are important for future analysis of the delay in high temporal resolution.

In our main analysis we confirmed the findings of previous studies dealing with variations of the delayed ionospheric response to solar EUV with solar activity and latitude. The variability of the delayed ionospheric response to solar EUV with geomagnetic activity and the seasonal variations of the delay was shown with delay time series from 2011 to 2013. These findings allow the following conclusions:

https://doi.org/10.5194/angeo-2019-91
Preprint. Discussion started: 8 July 2019

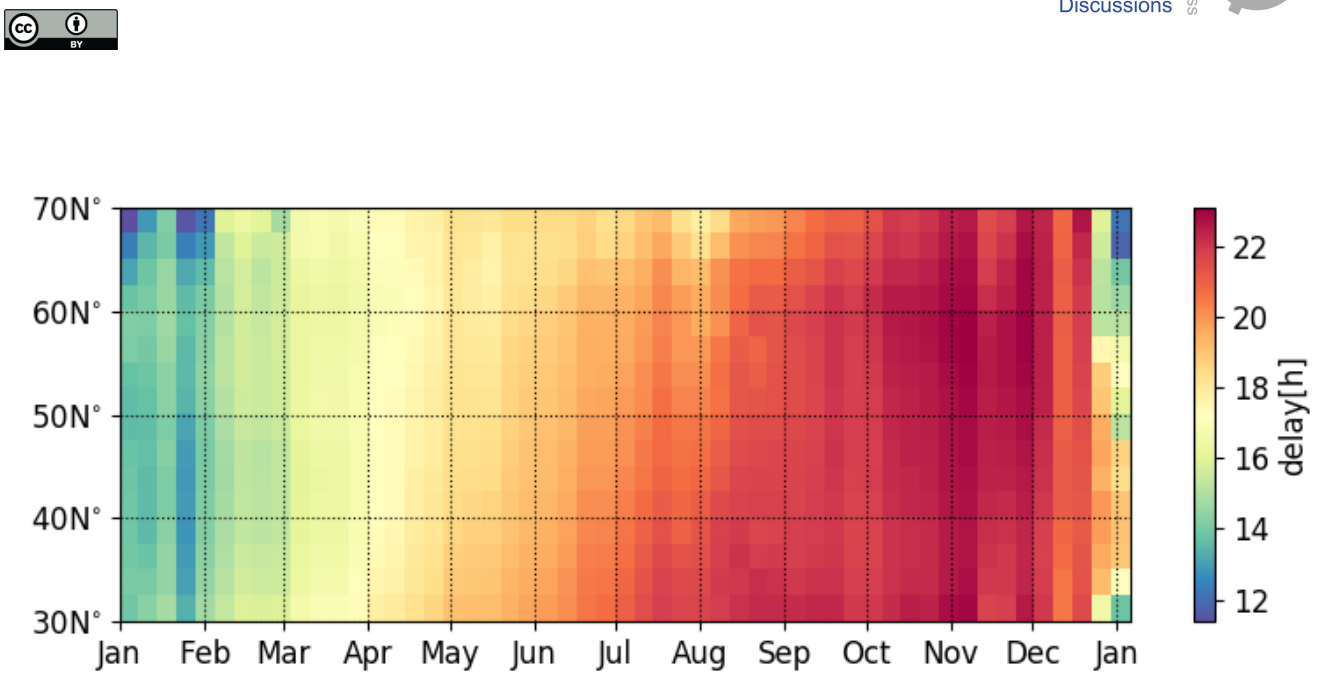

Figure 12. Time series of the delay of TEC with respect to EUV as an epoch plot for the mid-latitudes covering Europe within the time period from 2011 to 2013. The delay varies between ≈ 11.3 and ≈ 23.1 hours.

- The comparison of the delay for locations in northern and southern hemisphere shows a seasonal variation, which occurs for both investigated ionospheric parameters TEC and foF2. The seasonal variation for foF2, which describes only the F2 layer, is larger compared with TEC of the whole ionosphere-plasmasphere system.
- The analysis of IGS TEC maps covering the European region indicates a latitudinal dependence of the delay for mid-latitudes, which is pronounced in summer and vanishes in winter. A North-South trend of the ionospheric delay during summer month has been observed with ≈ 0.06 hours per degree in latitude.
- The geomagnetic activity has a strong influence on the delay, which is visible as global trend in the delay within this study. The strong impact of the geomagnetic activity was already suggested in other studies, e.g. Ren et al. (2018).
- The results indicate an influence of the 11-year solar cycle or at least an increase of the delay with increasing solar activity from year to year. This result is consistent with findings by Rich et al. (2003) and Chen et al. (2015).

For the seasonal variation the difference in the delay was calculated at stations of similar latitude in both hemispheres for TEC with $\approx 5 \pm 0.7$ hours and foF2 with $\approx 8 \pm 0.8$ hours. The decrease of the delay with latitude in the European mid-latitudes from ≈ 21.5 hours at 30°N to ≈ 19 hours at 70°N in summer and the roughly constant delay of ≈ 19.5 hours for the whole region in winter also show a seasonal difference in the delay.

In future analysis the delay should be calculated for even longer time periods in high temporal resolution covering different solar and geomagnetic activity conditions. This requires better and more EUV measurements though. In addition, the analysis of the influence of thermospheric conditions is important. Results presented need to be further confirmed and studied by model

https://doi.org/10.5194/angeo-2019-91
Preprint. Discussion started: 8 July 2019

245 calculations. The underlying processes for the delayed ionospheric response to solar EUV radiation need to be described, since this knowledge is an opportunity to validate or improve physics-based models.

Data availability. Kp-index data have been provided by NASA through https://omniweb.gsfc.nasa.gov/form/dx1.html.
IGS TEC maps have been provided by NASA through ftp://cddis.gsfc.nasa.gov/gnss/products/ionex.
Ionosonde data have been provided by NOAA ftp://ftp.ngdc.noaa.gov/ionosonde/. SDO-EVE data have been provided by LASP through
250 http://lasp.colorado.edu/eve/data_access/evewebdata.

Author contributions. E. Schmölter performed the calculations and composed the fist draft of the paper. J. Berdermann, N. Jakowski, and Ch. Jacobi actively contributed to the analysis and paper writing.

Competing interests. Ch. Jacobi is one of the editors-in-chief of Annales Geophysicae.

255 *Acknowledgements.* IGS TEC maps and Kp-index data have been provided by NASA. EVE data has been provided by LASP. Ionosonde data has been provided by NOAA. The study has been supported by Deutsche Forschungsgemeinschaft (DFG) through grants No. BE 5789/2-1 and JA 836/33-1.

https://doi.org/10.5194/angeo-2019-91
Preprint. Discussion started: 8 July 2019

Annales Geophysicae Discussions

References

Afraimovich, E. L., Astafyeva, E. I., Oinats, A. V., Yasukevich, Y. V., and Zhivetiev, I. V.: Global electron content: a new conception to track solar activity, Annales Geophysicae, 26, 335–344, https://doi.org/10.5194/angeo-26-335-2008, 2008.

Berdermann, J., Kriegel, M., Banyś, D., Heymann, F., Hoque, M. M., Wilken, V., Borries, C., Heßelbarth, A., and Jakowski, N.: Ionospheric Response to the X9.3 Flare on 6 September 2017 and Its Implication for Navigation Services Over Europe, Space Weather, 16, 1604–1615, https://doi.org/10.1029/2018sw001933, 2018.

Chen, Y., Liu, L., Le, H., and Zhang, H.: Discrepant responses of the global electron content to the solar cycle and solar rotation variations of EUV irradiance, Earth, Planets and Space, 67, 80, https://doi.org/10.1186/s40623-015-0251-x, 2015.

Chen, Y., Liu, L., Le, H., and Wan, W.: Responses of Solar Irradiance and the Ionosphere to an Intense Activity Region, Journal of Geophysical Research: Space Physics, 123, 2116–2126, https://doi.org/10.1002/2017JA024765, 2018.

Hernández-Pajares, M., Juan, J. M., Sanz, J., Orus, R., Garcia-Rigo, A., Feltens, J., Komjathy, A., Schaer, S. C., and Krankowski, A.: The IGS VTEC maps: a reliable source of ionospheric information since 1998, Journal of Geodesy, 83, 263–275, https://doi.org/10.1007/s00190-008-0266-1, 2009.

Hunsucker, R. D. and Hargreaves, J. K.: The High-Latitude Ionosphere and its Effects on Radio Propagation (Cambridge Atmospheric and Space Science Series), Cambridge University Press, 2002.

Jacobi, C., Jakowski, N., Schmidtke, G., and Woods, T. N.: Delayed response of the global total electron content to solar EUV variations, Advances in Radio Science, 14, 175–180, https://doi.org/10.5194/ars-14-175-2016, 2016.

Jakowski, N., Fichtelmann, B., and Jungstand, A.: Solar activity control of ionospheric and thermospheric processes, Journal of Atmospheric and Terrestrial Physics, 53, 1125 – 1130, https://doi.org/10.1016/0021-9169(91)90061-B, the 7th International Scostep symposium on Solar-Terrestrial Physics, 1991.

Jakowski, N., Heise, S., Wehrenpfennig, A., Schlüter, S., and Reimer, R.: GPS/GLONASS-based TEC measurements as a contributor for space weather forecast, Journal of Atmospheric and Solar-Terrestrial Physics, 64, 729–735, https://doi.org/10.1016/s1364-6826(02)00034-2, 2002.

LASP: EVE Data, http://lasp.colorado.edu/eve/data_access/evewebdata, last access 06.07.2019, 2019.

Lee, C.-K., Han, S.-C., Bilitza, D., and Seo, K.-W.: Global characteristics of the correlation and time lag between solar and ionospheric parameters in the 27-day period, Journal of Atmospheric and Solar-Terrestrial Physics, 77, 219 – 224, https://doi.org/10.1016/j.jastp.2012.01.010, 2012.

Machol, J., Viereck, R., and Jones, A.: GOES EUVS Measurements, 2016.

Min, K., Park, J., Kim, H., Kim, V., Kil, H., Lee, J., Rentz, S., Lühr, H., and Paxton, L.: The 27-day modulation of the low-latitude ionosphere during a solar maximum, Journal of Geophysical Research: Space Physics, 114, n/a–n/a, https://doi.org/10.1029/2008JA013881, a04317, 2009.

NASA: OMNIWeb, https://omniweb.gsfc.nasa.gov/form/dx1.html, last access 06.07.2019, 2019a.

NASA: Ionex products, ftp://cddis.gsfc.nasa.gov/gnss/products/ionex, last access 06.07.2019, 2019b.

Nikutowski, B., Brunner, R., Erhardt, C., Knecht, S., and Schmidtke, G.: Distinct EUV minimum of the solar irradiance (16–40nm) observed by SolACES spectrometers onboard the International Space Station (ISS) in August/September 2009, Advances in Space Research, 48, 899 – 903, https://doi.org/10.1016/j.asr.2011.05.002, 2011.

NOAA: Ionosonde products, ftp://ftp.ngdc.noaa.gov/ionosonde/, last access 06.07.2019, 2019.

https://doi.org/10.5194/angeo-2019-91
Preprint. Discussion started: 8 July 2019

Oinats, A. V., Ratovsky, K. G., and Kotovich, G. V.: Influence of the 27-day solar flux variations on the ionosphere parameters measured at Irkutsk in 2003–2005, Advances in Space Research, 42, 639 – 644, https://doi.org/10.1016/j.asr.2008.02.009, 2008.

Ren, D., Lei, J., Wang, W., Burns, A., Luan, X., and Dou, X.: Does the Peak Response of the Ionospheric F 2 Region Plasma Lag the Peak of 27-Day Solar Flux Variation by Multiple Days?, Journal of Geophysical Research: Space Physics, 123, 7906–7916, https://doi.org/10.1029/2018JA025835, 2018.

Rich, F. J., Sultan, P. J., and Burke, W. J.: The 27-day variations of plasma densities and temperatures in the topside ionosphere, Journal of Geophysical Research: Space Physics, 108, https://doi.org/10.1029/2002JA009731, 2003.

Rishbeth, H.: How the thermospheric circulation affects the ionospheric F2-layer, Journal of Atmospheric and Solar-Terrestrial Physics, 60, 1385 – 1402, https://doi.org/10.1016/S1364-6826(98)00062-5, 1998.

Rishbeth, H., Müller-Wodarg, I. C. F., Zou, L., Fuller-Rowell, T. J., Millward, G. H., Moffett, R. J., Idenden, D. W., and Aylward, A. D.: Annual and semiannual variations in the ionospheric F2-layer: II. Physical discussion, Annales Geophysicae, 18, 945–956, https://doi.org/10.1007/s00585-000-0945-6, 2000.

Schmidtke, G., Nikutowski, B., Jacobi, C., Brunner, R., Erhardt, C., Knecht, S., Scherle, J., and Schlagenhauf, J.: Solar EUV Irradiance Measurements by the Auto-Calibrating EUV Spectrometers (SolACES) Aboard the International Space Station (ISS), Solar Physics, 289, 1863–1883, https://doi.org/10.1007/s11207-013-0430-5, 2014.

Schmölter, E., Berdermann, J., Jakowski, N., Jacobi, C., and Vaishnav, R.: Delayed response of the ionosphere to solar EUV variability, Advances in Radio Science, 16, 149–155, https://doi.org/10.5194/ars-16-149-2018, 2018.

Titheridge, J. E.: The electron content of the southern mid-latitude ionosphere, 1965–1971, Journal of Atmospheric and Terrestrial Physics, 35, 981–1001, https://doi.org/10.1016/0021-9169(73)90077-9, 1973.

Unglaub, C., Jacobi, C., Schmidtke, G., Nikutowski, B., and Brunner, R.: EUV-TEC proxy to describe ionospheric variability using satellite-borne solar EUV measurements: First results, Advances in Space Research, 47, 1578 – 1584, https://doi.org/10.1016/j.asr.2010.12.014, 2011.

Woods, T. N., Eparvier, F. G., Bailey, S. M., Chamberlin, P. C., Lean, J., Rottman, G. J., Solomon, S. C., Tobiska, W. K., and Woodraska, D. L.: Solar EUV Experiment (SEE): Mission overview and first results, Journal of Geophysical Research: Space Physics, 110, n/a–n/a, https://doi.org/10.1029/2004JA010765, a01312, 2005.

Woods, T. N., Eparvier, F. G., Hock, R., Jones, A. R., Woodraska, D., Judge, D., Didkovsky, L., Lean, J., Mariska, J., Warren, H., McMullin, D., Chamberlin, P., Berthiaume, G., Bailey, S., Fuller-Rowell, T., Sojka, J., Tobiska, W. K., and Viereck, R.: Extreme Ultraviolet Variability Experiment (EVE) on the Solar Dynamics Observatory (SDO): Overview of Science Objectives, Instrument Design, Data Products, and Model Developments, Solar Physics, 275, 115–143, https://doi.org/10.1007/s11207-009-9487-6, 2012.

Wright, J. and Paul, A. K.: Toward Global Monitoring of the Ionosphere in Real Time by a Modern Ionosonde Network: The Geophysical Requirements and Technological Opportunity, Journal of Geophysical Research, 1981.

Zhang, S.-R. and Holt, J. M.: Ionospheric variability from an incoherent scatter radar long-duration experiment at Millstone Hill, Journal of Geophysical Research: Space Physics, 113, n/a–n/a, https://doi.org/10.1029/2007ja012639, 2008.

Zieger, B. and Mursula, K.: Annual variation in near-Earth solar wind speed: Evidence for persistent north-south asymmetry related to solar magnetic polarity, Geophysical Research Letters, 25, 841–844, https://doi.org/10.1029/98GL50414, 1998.